BIOCHEMISTRY
including biophysical chemistry & molecular biology

Accelerated Publication

pubs.acs.org/biochemistry

Conformational Selection or Induced Fit? A Critical Appraisal of the Kinetic Mechanism

Austin D. Vogt and Enrico Di Cera*

Edward A. Doisy Department of Biochemistry and Molecular Biology, Saint Louis University School of Medicine, St. Louis, Missouri 63104, United States

ABSTRACT: For almost five decades, two competing mechanisms of ligand recognition, conformational selection and induced fit, have dominated our interpretation of ligand binding in biological macromolecules. When binding−dissociation events are fast compared to conformational transitions, the rate of approach to equilibrium, k_{obs}, becomes diagnostic of conformational selection or induced fit based on whether it decreases or increases, respectively, with the ligand concentration, [L]. However, this simple conclusion based on the rapid equilibrium approximation is not valid in general. Here we show that conformational selection is associated with a rich repertoire of kinetic properties, with k_{obs} decreasing or increasing with [L] depending on the relative magnitude of the rate of ligand dissociation, k_{off}, and the rate of conformational isomerization, k_r. We prove that, even for the simplest two-step mechanism of ligand binding, a decrease in k_{obs} with [L] is unequivocal evidence of conformational selection, but an increase in k_{obs} with [L] is not unequivocal evidence of induced fit. Ligand binding to glucokinase, thrombin, and its precursor prethrombin-2 are used as relevant examples. We conclude that conformational selection as a mechanism for a ligand binding to its target may be far more common than currently believed.

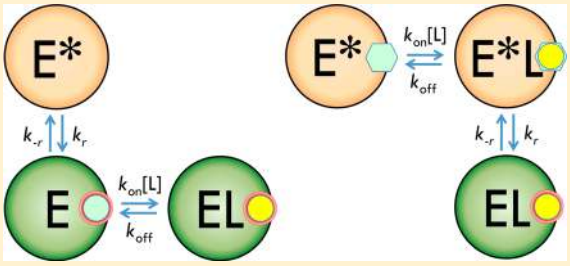

The specific encounter between a ligand and a host target is fundamental to the chemistry of all biological activities. Understanding the molecular mechanism of how ligands recognize their targets and how those interactions are regulated remains a central issue to biochemistry and biophysics and a critical prerequisite for our ability to rationally design effective drugs and new therapeutics.[1] In its simplest incarnation, binding of ligand L to its biological target E can be cast in terms of the single-step reaction scheme[2] (Scheme 1)

Scheme 1

$$\mathrm{E} \underset{k_{on}[\mathrm{L}]}{\overset{k_{off}}{\leftrightarrows}} \mathrm{E{:}L}$$

where k_{on} (M^{-1} s^{-1}) is the second-order rate constant for ligand binding and k_{off} (s^{-1}) is the first-order rate of dissociation of the E:L complex into the parent species E and L. The strength of the interaction is quantified by the equilibrium association constant K_a (M^{-1}) defined as the k_{on}/k_{off} ratio, or equivalently by the equilibrium dissociation constant K_d (M) defined as the inverse of K_a, or k_{off}/k_{on}. Scheme 1 provides an important starting point for any discussion of ligand binding but offers little insight into the mechanism of recognition. Basically, the scheme assumes that the binding interaction is a rigid body collision between the ligand and its target, with no conformational change involved. In this case, the system approaches equilibrium according to an observed rate constant, k_{obs}, that increases linearly with [L]. The set of differential equations associated with Scheme 1 is in fact

$$\begin{pmatrix} d[E]/dt \\ d[E{:}L]/dt \end{pmatrix} = \begin{pmatrix} -k_{on}[L] & k_{off} \\ k_{on}[L] & -k_{off} \end{pmatrix} \begin{pmatrix} [E] \\ [E{:}L] \end{pmatrix} \quad (1)$$

and the non-zero eigenvalue of the 2 × 2 matrix above gives the k_{obs} measured experimentally as

$$-\lambda_1 = k_{obs} = k_{off} + k_{on}[L] \quad (2)$$

A plot of k_{obs} versus [L] is linear with intercept k_{off} and slope k_{on}, from which the value of equilibrium association constant K_a or K_d can be easily derived.

Scheme 1 needs to be extended in the more realistic scenario of a binding interaction that involves conformational transitions. In this case, the rate of approach to equilibrium is no longer a linear function of [L]. Two limiting schemes become of interest as special cases of a more general scheme that links ligand binding to conformational transitions,[3,4] as shown in Figure 1. In the first case (Scheme 2), the target exists in distinct conformations in equilibrium and the ligand selects the one with an optimal fit

Received: May 25, 2012
Revised: June 19, 2012
Published: July 9, 2012

   dx.doi.org/10.1021/bi3006913 | *Biochemistry* 2012, 51, 5894−5902

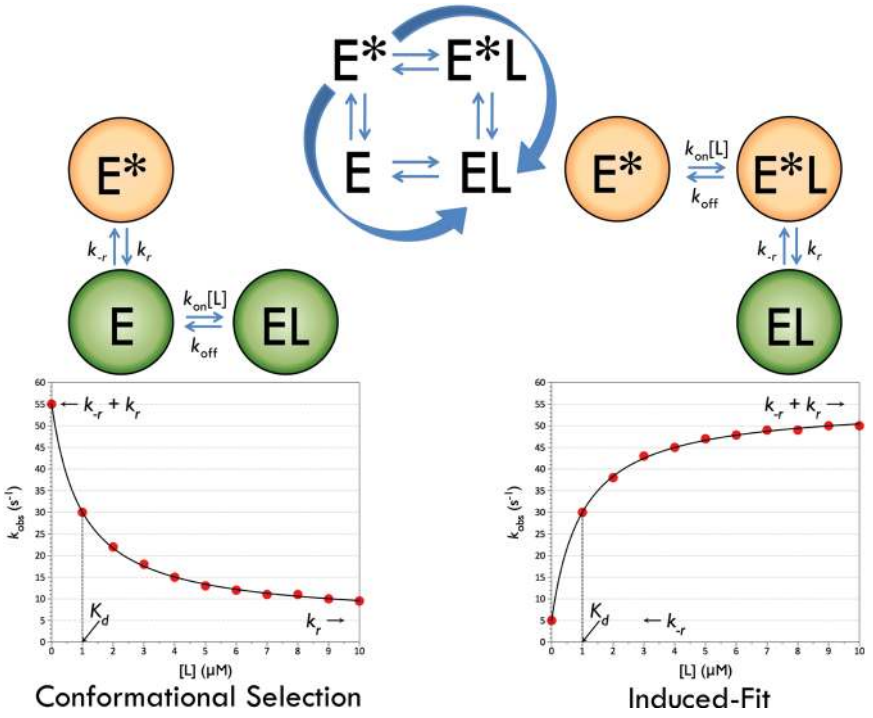

Figure 1. Conformational selection and induced fit. The two alternative mechanisms of ligand recognition in Schemes 2 (left) and 3 (right) show the different roles of conformational transitions in the binding process. The two schemes are special cases of a general scheme (middle) linking conformational changes to ligand binding. Conformational selection (derived from the pathway at the bottom left in the general scheme) postulates a preexisting equilibrium between the E* and E forms, of which only E binds the ligand. Under the rapid equilibrium approximation, the rate of approach to equilibrium, k_{obs}, is an inverse hyperbolic function of the ligand concentration from which the values of k_r and k_{-r} for the E*−E interconversion can be derived directly, along with the value of K_d for ligand binding. In this mechanism, the value of k_{obs} decreases with an increasing ligand concentration. The induced fit model (derived from the pathway at the top right in the general scheme) postulates a conformational transition between E*:L and E:L that optimizes binding. Under the rapid equilibrium approximation, the rate of approach to equilibrium, k_{obs}, is a hyperbolic function of the ligand concentration from which the values of k_r and k_{-r} for the E*:L−E:L interconversion can be derived directly, along with the value of K_d for ligand binding. In this mechanism, the value of k_{obs} increases with an increasing ligand concentration. Hence, under the rapid equilibrium approximation, the dependence of k_{obs} on ligand concentration [L] is diagnostic of the mechanism of binding.

Scheme 2

$$\mathrm{E^*} \underset{k_r}{\overset{k_{-r}}{\leftrightarrows}} \mathrm{E} \underset{k_{on}[\mathrm{L}]}{\overset{k_{off}}{\leftrightarrows}} \mathrm{E{:}L}$$

The species E* is added to reflect a preexisting equilibrium between two forms, E* and E, of which only E can interact with ligand L. The rate constants k_r and k_{-r} refer to the transitions from E* to E and backward, respectively, with the k_{-r}/k_r ratio (r) quantifying the population of E* relative to E. This is the simplest form of the celebrated Monod−Wyman−Changeux model of allosteric transitions.[5] In the second case (Scheme 3), the conformation of the target changes after ligand binding to provide an optimal fit

Scheme 3

$$\mathrm{E^*} \underset{k_{on}[\mathrm{L}]}{\overset{k_{off}}{\leftrightarrows}} \mathrm{E^*{:}L} \underset{k_r}{\overset{k_{-r}}{\leftrightarrows}} \mathrm{E{:}L}$$

In this case, the rate constants k_r and k_{-r} refer to the transition from E*:L to E:L and backward, respectively, with the k_{-r}/k_r ratio (r) quantifying the population of E*:L relative to E:L. Scheme 3 is the simplest form of the alternative Koshland−Nemethy−Filmer model of allosteric transitions[6] based on the induced-fit hypothesis.[7] Schemes 2 and 3 have long been considered mutually exclusive, and distinguishing between them continues to dominate discussions in several systems of interest to biology and chemistry.[4,8−10]

Under the "rapid equilibrium approximation", binding and dissociation steps in Schemes 2 and 3 are assumed to be fast compared to conformational changes[11,12] and the dependence of k_{obs} on [L] becomes diagnostic of the mechanism involved (Figure 1). In the case of Scheme 2, k_{obs} decreases hyperbolically with [L] according to the equation

$$k_{obs} = k_r + k_{-r}\frac{1}{1 + K_a[\mathrm{L}]} = k_r + k_{-r}\frac{K_d}{K_d + [\mathrm{L}]} \quad (3)$$

A plot of k_{obs} versus [L] is an inverse hyperbola with asymptotic values of $k_{-r} + k_r$ for [L] = 0 and k_r for [L] = ∞. The midpoint between these values defines the equilibrium constant K_d. The dependence of k_{obs} on [L] reflects the decrease in the number of species from two (E* and E) to one (EL) as [L] increases, with the rate of approach to equilibrium shifting from the reversible E*−E interconversion at low ligand concentrations, with a $k_{-r} + k_r$ value, to the irreversible E*−E conversion at high ligand concentrations

dx.doi.org/10.1021/bi3006913 | Biochemistry 2012, 51, 5894−5902

(rate k_r). In the case of Scheme 3, k_{obs} increases hyperbolically with [L] according to the equation

$$k_{obs} = k_{-r} + k_r\frac{K_a[L]}{1 + K_a[L]} = k_{-r} + k_r\frac{[L]}{K_d + [L]} \quad (4)$$

A plot of k_{obs} versus [L] is a rectangular hyperbola with asymptotic values of k_{-r} for [L] = 0 and $k_{-r} + k_r$ for [L] = ∞, and again the midpoint between these values defines the equilibrium constant K_d. In this case, the dependence of k_{obs} on [L] reflects the increase in the number of species from one (E*) to two (E*L and EL) as [L] increases, with the rate of approach to equilibrium shifting from the irreversible EL to E*L conversion at low ligand concentrations, with a value k_{-r}, to the reversible E*L−EL interconversion at high ligand concentrations (rate $k_{-r} + k_r$). The widely used rapid equilibrium approximation has fueled the notion that conformational selection (Scheme 2) and induced fit (Scheme 3) can easily be distinguished from the kinetics of approach to equilibrium.[11] In turn, the preponderance of experimental systems found to obey eq 4 relative to eq 3 has been cited as evidence that induced fit is the dominant mechanism of recognition in ligand binding to proteins.[11,13] In this study, we analyze the kinetics of approach to equilibrium for Schemes 2 and 3 without simplifying assumptions about the rate constants and show how information about the mechanism of recognition can be extracted from the plot of k_{obs} versus [L]. Our analysis calls for caution in the use of the rapid equilibrium approximation in the analysis of experimental data.

MATERIALS AND METHODS

Prethrombin-2 and thrombin were expressed in *Escherichia coli* and purified from inclusion bodies, essentially as described previously.[14,15] Both proteins were expressed with the S195A substitution, which renders the protein catalytically inert while leaving its binding properties intact.[16,17] Stopped-flow fluorescence measurements were conducted on an Applied Photophysics SX20 spectrometer using 1:1 mixing in a total volume of 60 μL. For Na^+, K^+, FPR, and VPR, the intrinsic fluorescence of thrombin was monitored with an excitation wavelength of 283 nm and a cutoff filter of 305 nm. The active site inhibitor *p*-aminobenzamidine (PABA) has a strong fluorescence signal at 380 nm when excited at 330 nm and shows extraordinary sensitivity to its binding environment in the active site of trypsin-like proteases;[18,19] thus, these experiments were conducted via excitation at 330 nm with a 375 nm cutoff filter, as described previously.[19] Final thrombin concentrations were 50 nM (Na^+ binding), 75 nM (VPR and FPR binding), 100 nM (K^+ binding), and 1 μM (PABA binding). All thrombin binding experiments were conducted in the presence of 5 mM Tris (pH 8.0) at 15 °C with 0.1% PEG8000, with an ionic strength kept constant at 400 mM with choline chloride. Prethrombin-2 (75 nM) used essentially the same buffer with pH 8.0 at the temperature of interest. Individual kinetic traces were determined by averaging a minimum of four traces each from three independent ligand titrations. Traces were fit to a single-exponential equation, with the quality of the fit determined by evaluation of the residuals. The k_{obs} values, taken from the single-exponential fits, were plotted against ligand concentration [L], and these plots were used for all subsequent fitting to various kinetic schemes. Best-fit parameter values were derived by a nonlinear least-squares method with Mathematica.

RESULTS

Consider Scheme 2 and the set of differential equations associated with it

$$\begin{pmatrix} d[E^*]/dt \\ d[E]/dt \\ d[E{:}L]/dt \end{pmatrix} = \begin{pmatrix} -k_r & k_{-r} & 0 \\ k_r & -k_{-r} - k_{on}[L] & k_{off} \\ 0 & k_{on}[L] & -k_{off} \end{pmatrix} \begin{pmatrix} [E^*] \\ [E] \\ [E{:}L] \end{pmatrix} \quad (5)$$

The two non-zero eigenvalues of the 3 × 3 matrix of kinetic rate constants are

$$-\lambda_{1,2} = \left[k_{-r} + k_r + k_{off} + k_{on}[L] \pm \sqrt{(k_{off} + k_{on}[L] - k_{-r} - k_r)^2 + 4k_{-r}k_{on}[L]}\right]/2 \quad (6)$$

In the general case, when no assumption is made about the relative rates of binding and conformational transition, the kinetics of approach to equilibrium depend on two exponentials, each associated with an observed rate constant defined by the solutions of eq 5. The larger eigenvalue, $-\lambda_1$, defines a k_{obs} that becomes increasingly fast as [L] increases. Detection of the contribution of this eigenvalue to the kinetics of approach to equilibrium may be difficult with standard transient kinetics and may require the use of ultrarapid techniques like continuous flow and temperature jump. The smaller eigenvalue, $-\lambda_2$, typically defines the evolution of the system over a time scale accessible to rapid kinetics technique like stopped flow. It is this eigenvalue that directly relates to the k_{obs} accessible to experimental measurements. Elementary rearrangements of eq 6 show that under the rapid equilibrium approximation ($k_{off} + k_{on}[L] \gg k_{-r} + k_r$) the larger eigenvalue $-\lambda_1$ is simply $k_{off} + k_{on}[L]$ and the smaller eigenvalue $-\lambda_2$ is given by eq 3 and decreases hyperbolically with [L]. We are interested in the behavior of eq 6 in the general case.

Consider how eq 6 depends on [L] and especially its limiting values for [L] = 0 and [L] = ∞ (Table 1). As [L] increases, $-\lambda_1$ grows linearly as $k_{on}[L]$ but $-\lambda_2$ approaches the asymptotic value of k_r. The limit for [L] = 0 depends on the difference $k_{off} - k_{-r} - k_r$. When the difference is positive ($k_{off} > k_{-r} + k_r$), then $-\lambda_1 = k_{off}$ and $-\lambda_2 = k_{-r} + k_r$. If the difference is negative ($k_{-r} + k_r > k_{off}$), then $-\lambda_1 = k_{-r} + k_r$ and $-\lambda_2 = k_{off}$. Basically, for [L] = 0, $-\lambda_1$ and $-\lambda_2$ assume the larger and smaller values, respectively, between k_{off} and the sum $k_{-r} + k_r$. When k_{off} exceeds the sum $k_{-r} + k_r$, the situation is analogous to the rapid equilibrium approximation where $-\lambda_1 = k_{off} + k_{on}[L]$ and $-\lambda_2$ is given by eq 3. However, when $k_{-r} + k_r$ exceeds k_{off}, the kinetics become dependent on the relative magnitude of k_{off} and k_r. When $k_{off} > k_r$, the value of $-\lambda_2 = k_{obs}$ decreases with [L]. Although this situation is analogous to the $k_{off} > k_{-r} + k_r$ case, there is an important distinction insofar as the asymptotic value for [L] = 0 does not give $k_{-r} + k_r$ as in the rapid equilibrium approximation but k_{off}. Hence, when $k_{-r} + k_r > k_{off} > k_r$, Scheme 2 produces a dependence of k_{obs} on [L] that can be mistaken with that observed under the rapid equilibrium approximation (Figure 2), with the asymptotic value of k_{obs} for [L] = 0 becoming incorrectly assigned as the sum $k_{-r} + k_r$ instead of k_{off}. It also follows from inspection of eq 6 that the value of $-\lambda_2 = k_{obs}$ does not change with [L] when $k_{off} = k_r$ (Figure 2). The lack of dependence of k_{obs} on [L] was originally reported in the first rapid kinetics study of binding of Na^+ to thrombin[20] and interpreted in terms of an extended version of Scheme 2. It is now clear that Scheme 2 used in its general form

dx.doi.org/10.1021/bi3006913 | *Biochemistry* 2012, 51, 5894−5902

Table 1. Kinetic Signatures of Conformational Selection and Induced Fit in the General Case

	conformational selection (Scheme 2)		induced fit (Scheme 3)
$-\lambda_{1,2}$	$\left[k_{-r} + k_r + k_{off} + k_{on}[L] \pm \sqrt{(k_{off} + k_{on}[L] - k_{-r} - k_r)^2 + 4k_{-r}k_{on}[L]}\right]/2$		$\left[k_{-r} + k_r + k_{off} + k_{on}[L] \pm \sqrt{(k_{off} + k_{on}[L] - k_{-r} - k_r)^2 + 4k_rk_{off}}\right]/2$
$-\lambda_1$ ([L] = 0)	k_{off}	$k_{off} > k_{-r} + k_r$	$k_{-r} + k_r + k_{off} + \sqrt{(k_{off} - k_{-r} - k_r)^2 + 4k_rk_{off}}\Big]/2$
		$k_{off} < k_{-r} + k_r$	$k_{on}[L]$
$-\lambda_1$ ([L] = ∞)	$k_{on}[L]$	$k_{on}[L]$	$\left[k_{-r} + k_r + k_{off} - \sqrt{(k_{off} - k_{-r} - k_r)^2 + 4k_rk_{off}}\right]/2 < k_{-r} + k_r$
$-\lambda_2$ ([L] = 0)	$k_{-r} + k_r$	k_{off}	
$-\lambda_2$ ([L] = ∞)	k_r	k_r	$k_{-r} + k_r$
$k_{obs} = -\lambda_2$	always decreases with [L]	decreases ($k_{off} > k_r$) or increases ($k_{off} < k_r$) with [L]	always increases with [L]
$K_{d,app}$[a]	$\frac{[E^*] + [E]}{[EL]} = \frac{k_{off}}{k_{on}}\left(\frac{k_r + k_{-r}}{k_r}\right) = K_d(1 + r)$		$\frac{[E]}{[E^*:L] + [E:L]} = \frac{k_{off}}{k_{on}}\left(\frac{k_r}{k_r + k_{-r}}\right) = K_d\left(\frac{1}{1 + r}\right)$

[a] $K_{d,app}$ is the only parameter accessible to experimental measurements of the system at equilibrium.[29] Its value depends on the intrinsic K_d and the k_{-r}/k_r ratio (r) for Schemes 2 and 3. Because two independent parameters, K_d and r, cannot be resolved from the single independent parameter, $K_{d,app}$, measurements of ligand binding at equilibrium cannot be used to distinguish between conformational selection or induced fit.

easily accounts for a value of k_{obs} that is independent of [L], and no extension is necessary. Finally, when $k_{off} < k_r$, the value of $-\lambda_2 = k_{obs}$ actually increases with [L] and mimics the dependence observed in the case of induced fit (Figures 1 and 2). In the general case, conformational selection (Scheme 2) produces a gamut of kinetic properties that include those uniquely pertaining to induced fit (Scheme 3) under the assumption of rapid equilibrium.

Unlike Scheme 2, Scheme 3 always produces eigenvalues that increase with [L]. Scheme 3 is associated with the set of differential equations

$$\begin{pmatrix} d[E^*]/dt \\ d[E^*:L]/dt \\ d[E:L]/dt \end{pmatrix} = \begin{pmatrix} -k_{on}[L] & k_{off} & 0 \\ k_{on}[L] & -k_r - k_{off} & k_{-r} \\ 0 & k_r & -k_{-r} \end{pmatrix} \begin{pmatrix} [E^*] \\ [E^*:L] \\ [E:L] \end{pmatrix} \tag{7}$$

The two non-zero eigenvalues associated with the 3 × 3 matrix of kinetic rate constants are

$$-\lambda_{1,2} = \Big[k_{-r} + k_r + k_{off} + k_{on}[L] \pm \sqrt{(k_{off} + k_{on}[L] - k_{-r} - k_r)^2 + 4k_rk_{off}}\Big]/2 \tag{8}$$

There is a basic similarity between eqs 6 and 8, which differ only in the last term under the square root expression. However, this difference results in two eigenvalues that always increase with [L]. Unlike Scheme 2, there is no finite value of the rate constants in Scheme 3 that makes $-\lambda_2$ independent of [L]. As [L] increases, $-\lambda_1$ grows linearly as $k_{on}[L]$ as in the case of Scheme 2, but $-\lambda_2$ approaches the asymptotic value of $k_{-r} + k_r$. The limit for [L] = 0 does not depend on the relative values of k_{off} and the sum $k_{-r} + k_r$ (Table 1) as in Scheme 2 and is always less than the value reached for [L] = ∞. This implies that Scheme 3 always produces values of k_{obs} that increase with [L], as opposed to Scheme 2 that produces values of k_{obs} that decrease with, increase with, or are independent of [L] depending on the relative values of k_{off} and k_r.

A plot of k_{obs} decreasing with [L] or independent of [L] is unambiguous proof of conformational selection (Scheme 2), but a plot of k_{obs} increasing with [L] may also be associated with conformational selection (Figure 2) and cannot be considered unambiguous proof of induced fit (Scheme 3). Glucokinase illustrates this scenario directly. The enzyme was originally assumed to bind glucose at a single site according to induced fit[21] based on the analysis of rapid kinetics data where both the larger and smaller eigenvalues were resolved experimentally (Figure 3). The larger eigenvalue produces a k_{obs} that increases linearly with [L], and the smaller eigenvalue shows a hyperbolic increase with [L] as expected of Scheme 3 under the rapid equilibrium approximation. However, the data in Figure 3 cannot be considered unequivocal evidence of induced fit because they fit accurately to Scheme 2 without the rapid equilibrium approximation with the following rate constants: $k_{-r} = 7.16\ s^{-1}$, $k_r = 0.8\ s^{-1}$, $k_{off} = 0.34\ s^{-1}$, and $k_{on} = 540\ M^{-1}\ s^{-1}$. It comes as no surprise, then, that more recent kinetic measurements of binding of glucose to glucokinase support conformational selection over induced fit,[22] and it is now accepted that glucokinase exists in alternative conformations in equilibrium prior to the binding of any ligands.[23] This conclusion is strongly supported by recent X-ray structures of glucokinase that reveal how ligand binding

dx.doi.org/10.1021/bi3006913 | Biochemistry 2012, 51, 5894−5902

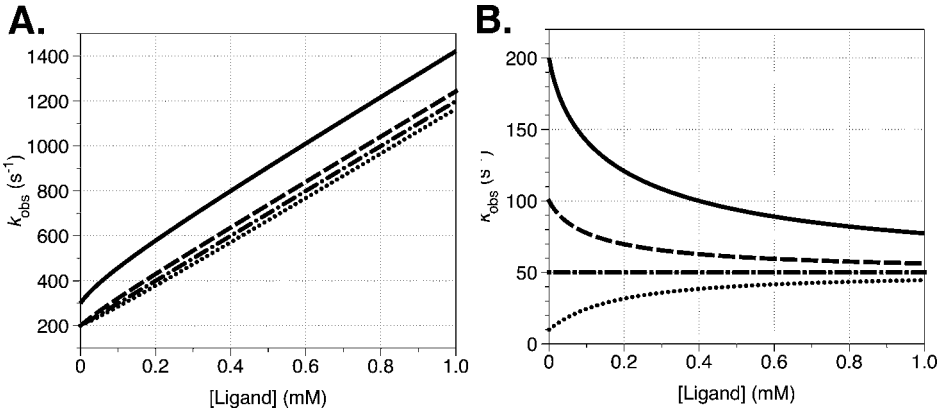

Figure 2. Dependence of k_{obs} on [L] for conformational selection. The eigenvalues $-\lambda_1$ (A) and $-\lambda_2$ (B) were simulated according to eq 6 in the text, with the following rate constants: $k_r = 50\ s^{-1}$, $k_{-r} = 150\ s^{-1}$, and $k_{on} = 10^6\ M^{-1}\ s^{-1}$ and k_{off} varied among $300\ s^{-1}$ (—), $100\ s^{-1}$ (– – –), $50\ s^{-1}$ (–·–), and $10\ s^{-1}$ (···). When $k_{off} > k_r + k_{-r}$ (—), the asymptotes of the curves in panels A and B are equivalent to those of eqs 2 and 3, respectively, under the rapid equilibrium approximation. However, when $k_r + k_{-r} > k_{off} > k_r$ (– – –), the values of $-\lambda_1$ and $-\lambda_2$ in the limit of [L] = 0 switch, with $k_r + k_{-r}$ defining the lower limit of $-\lambda_1$ and k_{off} defining the lower limit of $-\lambda_2$ (Table 1). When $k_{off} > k_r$ (— and – – –), the inverse hyperbola traditionally associated with conformational selection is retained and the curve will look essentially the same as predicted from eq 3. Importantly, when $k_r > k_{off}$ (···), the value of $-\lambda_2$ actually increases with ligand concentration, mimicking the behavior observed under the induced-fit mechanism (see Figure 1). The transition between the opposite dependencies of k_{obs} vs [L] is observed for $k_r = k_{off}$ (–·–), where k_{obs} is finite but independent of [L].

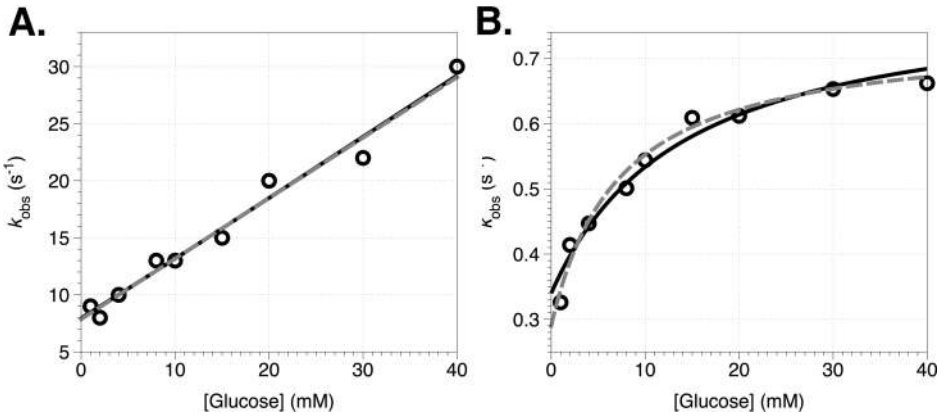

Figure 3. Rapid kinetics of binding of glucose to glucokinase. Data were taken from ref 21 and analyzed as in the original report according to the induced fit mechanism (gray dashed lines) under the rapid equilibrium approximation (eqs 2 and 3) with the following best-fit parameter values: $k_{on} = 530 \pm 30\ M^{-1}\ s^{-1}$, $k_{off} = 7.9 \pm 0.6\ s^{-1}$, $k_r = 0.45 \pm 0.03\ s^{-1}$, and $k_{-r} = 0.29 \pm 0.03\ s^{-1}$. These values are practically identical to those published by Heredia et al.[21] However, the same data can be fit according to the conformational selection mechanism (black lines) in the general case (eqs 5 and 6) with the following best-fit parameter values: $k_{on} = 540 \pm 30\ M^{-1}\ s^{-1}$, $k_{off} = 0.34 \pm 0.03\ s^{-1}$, $k_r = 0.80 \pm 0.06\ s^{-1}$, and $k_{-r} = 7.2 \pm 0.3\ s^{-1}$. Although the fits are equivalent in the two cases, they produce a very different description of the glucokinase–glucose interaction. The value of $K_{d,app}$ (Table 1) is similar in the two cases (9.1 and 6.3 mM, respectively), but the values of K_d reflecting the intrinsic binding affinity of glucose for glucokinase are 15 mM in the case of induced fit and 0.63 mM in the case of conformational selection. Induced fit predicts a weak binding interaction of glucose to glucokinase that is modestly strengthened by conformational rearrangements of the initial complex. On the other hand, conformational selection predicts tighter binding of glucose to the E form of glucokinase, with the resulting apparent affinity weakened by the significant population of E*.

does not result in conformational changes of the enzyme but only in stabilization of the E form.[24]

Figure 4 shows the values of k_{obs} as a function of [L] for the case of different ligands binding to the clotting protease thrombin.[25] The active site inhibitor PABA shows an inverse hyperbolic dependence of k_{obs} on [L] conforming to conformational selection according to Scheme 2. Under the rapid equilibrium approximation for PABA binding, analysis of the data in Figure 2 gives values a k_r of $74\ s^{-1}$ and a k_{-r} of $344\ s^{-1}$ for the E*–E interconversion, along with a K_d of 53 μM for the equilibrium association constant, which translates into $K_{d,app} = K_d(1 + r) = 300\ \mu M$ in agreement with equilibrium titration measurements.[18] The kinetic features of binding of PABA to thrombin show evidence of the E*–E equilibrium in the free form of the enzyme. As for glucokinase, this conclusion is directly supported by X-ray structural data.[19] Thrombin crystallizes in the free form in two alternative conformations, one (E form) with the active site open and accessible to substrates and inhibitors like PABA and the other (E* form) with the active site occluded by a collapse of the segment of residues 215–217 that precludes binding of substrates or inhibitors like PABA. The E* and E forms have been detected crystallographically in the same protein construct for several thrombin mutants,[19] as well in numerous other members of the trypsin family.[26] Indeed, conformational selection is the dominant mechanism of ligand recognition in this large family of biologically important enzymes.[10]

Because the E*–E equilibrium exists in solution independent of any binding event, its presence should be detected with exactly

dx.doi.org/10.1021/bi3006913 | *Biochemistry* 2012, 51, 5894–5902

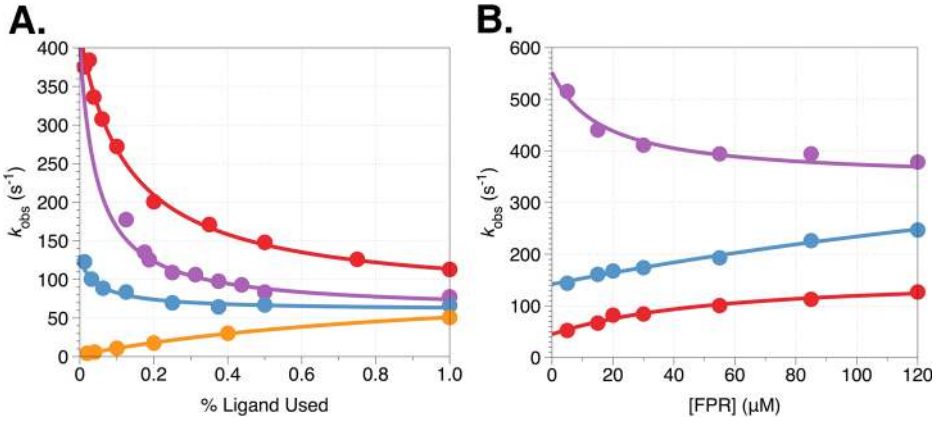

Figure 4. Rapid kinetics of binding of ligand to thrombin. (A) Rates of approach to equilibrium, k_{obs}, determined from stopped-flow fluorescence measurements of binding of PABA (red), KCl (magenta), NaCl (cyan), and VPR (orange) to thrombin, in 5 mM Tris and 0.1% PEG 8000 (pH 8.0) at 15 °C. The KCl and NaCl concentrations were changed by keeping the ionic strength constant at 400 mM with choline chloride, which was also used in the buffers for PABA and VPR. Solid lines were drawn according to eq 3 (PABA and K^+) or eq 6 (Na^+ and VPR), as described in Materials and Methods, with best-fit parameter values listed in Table 2. In all cases, the asymptotic value of k_{obs} for high ligand concentrations, k_r, levels off around 70 s^{-1}. On the other hand, the value of k_{obs} for [L] = 0 changes for different ligands and measures the sum $k_r + k_{-r}$ (PABA and K^+) or the value of k_{off} for ligand dissociation that exceeds (Na^+) or remains below (VPR) k_r. To facilitate comparison, the values of [L] for each ligand are expressed as a percentage of the maximal concentration used. (B) Rates of approach to equilibrium, k_{obs}, determined from stopped-flow fluorescence measurements of binding of FPR to prethrombin-2 at 15 (red), 25 (cyan), and 35 °C (magenta), in 5 mM Tris, 400 mM choline chloride, and 0.1% PEG 8000 (pH 8.0). The contrast in the dependence of k_{obs} on [L] between 15 and 25 °C (increase) and 35 °C (decrease) is easily explained by a temperature change in k_{off} that exceeds that of k_r (see also the simulation in Figure 2). Use of Scheme 2 in the general case, however, prevents resolution of the four independent parameters in eq 6 at each temperature, although it provides an excellent fit of the data (solid lines) when the values of k_{on} is arbitrarily fixed to 10^7 M^{-1} s^{-1}.

Table 2. Kinetic Parameters for Binding of Ligands to Thrombin

ligand	k_{on} (M^{-1} s^{-1})	k_{off} (s^{-1})	k_r (s^{-1})	k_{-r} (s^{-1})	K_d (M)	r	$K_{d,app}$ (M)
PABA	ND[a]	ND[a]	70 ± 10	340 ± 10	(5.2 ± 0.8) × 10^{-5}	4.9 ± 0.6	(2.9 ± 0.4) × 10^{-4}
Na^+	(3.2 ± 0.3) × 10^4	130 ± 20	60 ± 10	340 ± 10	(4.1 ± 0.4) × 10^{-3}	5.7 ± 0.7	(27 ± 4) × 10^{-3}
K^+	ND[a]	ND[a]	60 ± 10	340 ± 10	(19 ± 2) × 10^{-3}	5.7 ± 0.7	(130 ± 10) × 10^{-3}
VPR	(1.7 ± 0.1) × 10^7	2.4 ± 0.2	80 ± 10	340 ± 10	(1.4 ± 0.1) × 10^{-7}	4.3 ± 0.7	(7.5 ± 0.8) × 10^{-7}

[a]Not determined.

the same kinetic signatures regardless of the ligand under study. Specifically, different ligands influenced directly by the E*−E equilibrium should produce the same dependence of k_{obs} on [L] as seen for PABA (Figure 4), with identical asymptotic values for [L] = 0 and [L] = ∞. A key property of thrombin is its ability to bind monovalent cations like Na^+ and K^+ to a site near the primary specificity pocket that is obliterated by the repositioning of an Arg side chain when the enzyme switches from the E to the E* form.[25] Consistent with the scenario supported by structural data, binding of K^+ produces a dependence of k_{obs} on [L] that closely resembles that observed for PABA (Figure 4), thereby supporting the conclusion that the asymptotic values of k_{obs} for [L] = 0 and [L] = ∞ reflect the properties of the E*−E interconversion. However, binding of Na^+ deviates from binding of K^+ and PABA, especially in the asymptotic value of k_{obs} for [L] = 0 that defines the value of $k_r + k_{-r}$ (Table 1). Why do K^+ and Na^+ produce different asymptotic values of k_{obs} for [L] = 0 if they bind to the same site[27,28] and according to the same kinetic mechanism? A fourth ligand, the chromogenic substrate VPR binding to the active site like PABA, produces a dependence of k_{obs} on [L] that departs even more drastically from the profile seen for PABA and K^+ (Figure 4). In this case, the value of k_{obs} actually increases with [L]. The properties of Scheme 2 in the general case rationalize the seemingly disparate behavior observed in the binding of different ligands to thrombin (Figure 4). Binding of PABA, Na^+, and K^+ is consistent with the E*−E equilibrium, with only E allowing binding at the active site and the cation binding site, as indicated by structural biology.[19] For all ligands, the value of k_{obs} levels off around 70 s^{-1} at high ligand concentrations and increases to 400 s^{-1} for [L] = 0 for PABA and K^+ and 130 s^{-1} for Na^+. When k_{obs} decreases with [L], the value for [L] = 0 always measures whichever is smaller between k_{off} and the sum $k_{-r} + k_r$ (Table 1). Hence, the value of 130 s^{-1} measured for Na^+ binding at [L] = 0 should not be assigned to $k_{-r} + k_r$ but to k_{off} for Na^+ dissociation, and the value of 400 s^{-1} measured for PABA and K^+ binding is most likely the sum $k_{-r} + k_r$. These values allow assignement of a k_r of 70 s^{-1} and a k_{-r} of 340 s^{-1} (Table 2), making the E* form 5-fold more populated than E under the experimental conditions of the rapid kinetics measurements. Assignment of the asymptotic value of k_{obs} at [L] = 0 for Na^+ binding as the sum $k_{-r} + k_r$ would give a k_r of 60 s^{-1} and a k_{-r} of 67 s^{-1}, thereby making E* and E equally populated. This is the conclusion that was drawn in previous studies where the value of k_{obs} for [L] = 0 was interpreted as $k_r + k_{-r}$ under the assumption of rapid equilibrium for Na^+ binding.[19,29,30] The analysis presented here demonstrates that previous studies have underestimated the contribution of E* and supports the need for measurements involving different ligands, under the same solution conditions, to fully explore the range of k_{obs} values at the limits [L] = 0 and [L] = ∞ when the larger eigenvalue is not accessible to experimental measurements. Once the values of k_r and k_{-r} are assigned from measurements of PABA and K^+

dx.doi.org/10.1021/bi3006913 | *Biochemistry* 2012, 51, 5894−5902

binding, all other rate constants in eq 6 can be assigned for Na^+ (Table 2). The k_{on} value of $3.2 \times 10^4\ M^{-1}\ s^{-1}$ is in agreement with that determined from continuous-flow ultrarapid kinetics,[31] and the $K_{d,app} = K_d(1 + r) = 27$ mM relation agrees with equilibrium titrations of Na^+ binding.[32,33] In the case of the chromogenic substrate VPR, the value of k_{obs} at high ligand concentrations levels off around 70 s^{-1}, again in keeping with the rate for the E*−E transition (k_r), but the dependence of k_{obs} is drastically different and shows an increase with [L]. This behavior could be easily interpreted in terms of an induced fit under the rapid equilibrium approximation. On the other hand, Scheme 2 offers an alternative explanation in terms of conformational selection with k_{off} being much smaller than k_r, resulting in the following values: $k_{on} = 1.7 \times 10^7\ M^{-1}\ s^{-1}$, and $K_{d,app} = K_d(1 + r) = 0.75\ \mu M$ (consistent with previous kinetic[34] and equilibrium[17] measurements). Binding of four different ligands (PABA, K^+, Na^+, and VPR) to thrombin supports the same mechanism of conformational selection, even though the kinetic signatures differ drastically in the four cases.

Screening multiple ligands is a specific example of the more general strategy of altering the relative rates of k_r and k_{off} to differentiate between potential mechanisms and detect signatures of conformational selection. Perturbations that alter the values of k_{off} relative to k_r for the same ligand produce similar results. We demonstrate this principle with prethrombin-2,[15] an inactive zymogen precursor of thrombin, binding to the chromogenic substrate FPR at different temperatures. Because temperature may affect the values of k_{off} and k_r to different extents, it may be ideally suited to detection of drastic changes in the dependence of k_{obs} on [L]. At 15 °C, FPR binding displays the same hyperbolically increasing dependence of k_{obs} on [L] seen with VPR in thrombin, with asymptotes of 45 s^{-1} at [L] = 0 and 156 s^{-1} at [L] = ∞. Both the [L] = 0 and the [L] = ∞ asymptotes, reflecting k_{off} and k_r, respectively, increase with temperature but to different extents. At 25 °C, the asymptotes increase to 142 and 255 s^{-1} at the limits of [L] = 0 and [L] = ∞, respectively. However, at 35 °C, k_{off} becomes at least 550 s^{-1} and faster than k_r (365 s^{-1}), causing the dependence of k_{obs} on [L] to invert and decrease hyperbolically with [L] (Figure 4). Under the rapid equilibrium approximation, this type of behavior could be explained only by the mechanism of binding switching from induced fit at or below 25 °C to conformational selection at 35 °C, a very unrealistic scenario. On the other hand, Scheme 2 in the general case explains the binding of FPR to prethrombin-2 with a single mechanism, conformational selection, with the dependence of k_{obs} on [L] changing drastically based on the relative values of k_r and k_{off} at different temperatures, in keeping with the simulations reported in Figure 2. Hence, conformational selection applies not only to the mature enzyme thrombin but also to its inactive precursor prethrombin-2, thereby confirming kinetically well-established results from structural biology for thrombin[15] and trypsin-like proteases in general.[10,26]

DISCUSSION

A previous study by Galletto et al.[35] merged the mechanisms in Schemes 2 and 3 to produce a three-step scheme of ligand binding in which a preexisting equilibrium is followed by ligand-induced conformational changes. Because of the algebraic complexity of the expressions involved, the properties of such a scheme were analyzed under separate time scales. Important conclusions were reached about the dependence of k_{obs} on [L] and how the extended scheme would account for kinetic properties often associated with induced fit. A more recent study by Hammes et al.[4] offered a description of Schemes 2 and 3 in terms of fluxes along selected pathways of a more general scheme encompassing conformational transitions and ligand binding (Figure 1). A continuum version of that scheme has been discussed by Zhou.[9] Again, a richer repertoire of kinetic properties was identified for conformational selection. Our study reveals the kinetic properties of Schemes 2 and 3 and derives mathematical expressions for extracting rate constants from the analysis of experimental data. Conformational selection is shown to produce kinetic properties such as an increase in k_{obs} with [L] that overlap with those of induced fit, even though no such mechanism is present in Scheme 2. On the other hand, induced fit (Scheme 3) is unable to produce kinetic properties pertaining uniquely to conformational selection, i.e., a k_{obs} decreasing with [L] or independent of [L].

When the rapid equilibrium approximation is invoked, both Schemes 2 and 3 depend on three independent parameters (eqs 3 and 4) that can be resolved from a plot of k_{obs} versus [L]. If the approximation is not used, both schemes depend on four independent rate constants but the plot of k_{obs} versus [L] contains information about only three independent variables, i.e., the asymptotic values at [L] = 0 and [L] = ∞ and the midpoint of the transition. In this case, it is not possible to unequivocally resolve all the independent rate constants (k_r, k_{-r}, k_{on}, and k_{off}). The value of k_r for Scheme 2 is always defined by k_{obs} for high ligand concentrations, but the value at [L] = 0 is the smaller of $k_r + k_{-r}$ and k_{off}. The midpoint of the transition is not necessarily related to K_d. The situation is even more complex in the case of Scheme 3, where the value of k_{obs} for high ligand concentrations is $k_r + k_{-r}$ but the value for [L] = 0 depends on three rate constants (Table 1), and again the midpoint of the transition does not depend on only K_d. Determination of all four independent rate constants is always possible when both the larger and smaller eigenvalues are accessed experimentally, as shown in the case of glucokinase (Figure 3). However, this approach may not be feasible in general. Use of different ligands binding with different rate constants becomes essential, as shown in this study for thrombin. Although the approach in the general case may fail to provide the exact magnitude of the rate constants involved in the scheme, it is nonetheless instrumental in avoiding potentially incorrect conclusions based on the rapid equilibrium approximation. Particularly important is the need to assign the mechanism of binding when k_{obs} increases with [L], which cannot be linked unambiguously to induced fit as shown by our analysis and previous work.[4,35] In a recent review, Tummino and Copeland pointed out that induced fit is by far the most common mechanism of recognition documented experimentally, with conformational selection being confined to a handful of cases.[11] This conclusion was based on the results of kinetics analyzed under the rapid equilibrium approximation. Conformational selection can explain an increase of k_{obs} with [L] commonly assigned to induced fit, but induced fit can never account for a decrease in k_{obs} with [L] that unequivocally identifies conformational selection. We therefore suspect that the preponderance of induced fit as a mechanism of ligand binding needs to be critically reconsidered. Indeed, several proteins like alkaline phosphatase,[36] chymotrypsin,[12,37] thrombin,[20,29] meizothrombin-desF1,[38] glucokinase,[22] trypsin,[39] immunoglobulin IgE,[40] clotting proteases factor Xa, and activated protein C[30] obey conformational selection, and so does DNA in its B to Z transition.[41] Structural biology offers unequivocal evidence of multiple conformations in preexisting equilibrium for maltose-binding protein,[42] trypsin-like proteases in general,[10,26] and RNA.[43]

dx.doi.org/10.1021/bi3006913 | Biochemistry 2012, 51, 5894−5902

Our work offers a clear explanation for the apparent infrequency of conformational selection.[11] There is a lower limit on the equilibrium dissociation constant K_d where the characteristic inverse hyperbola of conformational selection will be detectable. As discussed earlier, the strength of a ligand binding interaction is controlled by the interplay between k_{on} and k_{off}, with the diffusion limit setting the upper bound for k_{on} at around 6.5×10^8 M^{-1} s^{-1}.[44] Because k_{on} is limited and k_{off} must exceed k_r for conformational selection to be detected, only ligands binding with

$$K_d > \frac{k_r}{k_{on}} \quad (9)$$

would produce a plot of k_{obs} that decreases hyperbolically with [L]. If the value of k_r is in the range of 100 s^{-1}, conformational selection can be detected only for K_d values of >150 nM, provided the ligand binds at the diffusion-limited rate. Thus, sampling multiple ligands is important for establishing the kinetic mechanism of binding, and experiments should be designed to sample conditions under which ligand binding is relatively weak.

AUTHOR INFORMATION

Corresponding Author

*Department of Biochemistry and Molecular Biology, Saint Louis University School of Medicine, St. Louis, MO 63104. Telephone: (314) 977-9201. Fax: (314) 977-1183. E-mail: enrico@slu.edu.

Funding

This work was supported in part by National Institutes of Health Grants HL49413, HL73813, HL95315, and HL112303.

Notes

The authors declare no competing financial interest.

ACKNOWLEDGMENTS

We are grateful to Ms. Tracey Baird for her help with the illustrations.

ABBREVIATIONS

FPR, H-D-Phe-Pro-Arg-*p*-nitroanilide; PABA, *p*-aminobenzamidine; PEG, polyethylene glycol; VPR, H-D-Val-Pro-Arg-*p*-nitroanilide.

REFERENCES

(1) Swinney, D. C. (2004) Biochemical mechanisms of drug action: What does it take for success? *Nat. Rev. Drug Discovery 3*, 801−808.

(2) Wyman, J., and Gill, S. J. (1990) *Binding and Linkage*, University Science Books, Mill Valley, CA.

(3) Hill, T. L. (1977) *Free Energy Transduction in Biology*, Academic Press, New York.

(4) Hammes, G. G., Chang, Y. C., and Oas, T. G. (2009) Conformational selection or induced fit: A flux description of reaction mechanism. *Proc. Natl. Acad. Sci. U.S.A. 106*, 13737−13741.

(5) Monod, J., Wyman, J., and Changeux, J. P. (1965) On the nature of allosteric transitions: A plausible model. *J. Mol. Biol. 12*, 88−118.

(6) Koshland, D. E., Jr., Nemethy, G., and Filmer, D. (1966) Comparison of experimental binding data and theoretical models in proteins containing subunits. *Biochemistry 5*, 365−385.

(7) Koshland, D. E. (1958) Application of a Theory of Enzyme Specificity to Protein Synthesis. *Proc. Natl. Acad. Sci. U.S.A. 44*, 98−104.

(8) Changeux, J. P., and Edelstein, S. (2011) Conformational selection or induced fit? 50 years of debate resolved. *Biol. Rep. 3*, 19.

(9) Zhou, H. X. (2010) From induced fit to conformational selection: A continuum of binding mechanism controlled by the timescale of conformational transitions. *Biophys. J. 98*, L15−L17.

(10) Pozzi, N., Vogt, A. D., Gohara, D. W., and Di Cera, E. (2012) Conformational selection in trypsin-like proteases. *Curr. Opin. Struct. Biol.*, 10.1016/j.sbi.2012.05.006.

(11) Tummino, P. J., and Copeland, R. A. (2008) Residence time of receptor-ligand complexes and its effect on biological function. *Biochemistry 47*, 5481−5492.

(12) Fersht, A. R. (1999) *Enzyme Structure and Mechanism*, Freeman, New York.

(13) Johnson, K. A. (2008) Role of induced fit in enzyme specificity: A molecular forward/reverse switch. *J. Biol. Chem. 283*, 26297−26301.

(14) Marino, F., Pelc, L. A., Vogt, A., Gandhi, P. S., and Di Cera, E. (2010) Engineering thrombin for selective specificity toward protein C and PAR1. *J. Biol. Chem. 285*, 19145−19152.

(15) Pozzi, N., Chen, Z., Zapata, F., Pelc, L. A., Barranco-Medina, S., and Di Cera, E. (2011) Crystal structures of prethrombin-2 reveal alternative conformations under identical solution conditions and the mechanism of zymogen activation. *Biochemistry 50*, 10195−10202.

(16) Stone, S. R., and Le Bonniec, B. F. (1997) Inhibitory mechanism of serpins. Identification of steps involving the active-site serine residue of the protease. *J. Mol. Biol. 265*, 344−362.

(17) Krem, M. M., and Di Cera, E. (2003) Dissecting substrate recognition by thrombin using the inactive mutant S195A. *Biophys. Chem. 100*, 315−323.

(18) Evans, S. A., Olson, S. T., and Shore, J. D. (1982) p-Aminobenzamidine as a fluorescent probe for the active site of serine proteases. *J. Biol. Chem. 257*, 3014−3017.

(19) Niu, W., Chen, Z., Gandhi, P. S., Vogt, A. D., Pozzi, N., Pelc, L. A., Zapata, F. J., and Di Cera, E. (2011) Crystallographic and kinetic evidence of allostery in a trypsin-like protease. *Biochemistry 50*, 6301−6307.

(20) Lai, M. T., Di Cera, E., and Shafer, J. A. (1997) Kinetic pathway for the slow to fast transition of thrombin. Evidence of linked ligand binding at structurally distinct domains. *J. Biol. Chem. 272*, 30275−30282.

(21) Heredia, V. V., Thomson, J., Nettleton, D., and Sun, S. (2006) Glucose-induced conformational changes in glucokinase mediate allosteric regulation: Transient kinetic analysis. *Biochemistry 45*, 7553−7562.

(22) Kim, Y. B., Kalinowski, S. S., and Marcinkeviciene, J. (2007) A pre-steady state analysis of ligand binding to human glucokinase: Evidence for a preexisting equilibrium. *Biochemistry 46*, 1423−1431.

(23) Antoine, M., Boutin, J. A., and Ferry, G. (2009) Binding kinetics of glucose and allosteric activators to human glucokinase reveal multiple conformational states. *Biochemistry 48*, 5466−5482.

(24) Petit, P., Antoine, M., Ferry, G., Boutin, J. A., Lagarde, A., Gluais, L., Vincentelli, R., and Vuillard, L. (2011) The active conformation of human glucokinase is not altered by allosteric activators. *Acta Crystallogr. D67*, 929−935.

(25) Di Cera, E. (2008) Thrombin. *Mol. Aspects Med. 29*, 203−254.

(26) Gohara, D. W., and Di Cera, E. (2011) Allostery in trypsin-like proteases suggests new therapeutic strategies. *Trends Biotechnol. 29*, 577−585.

(27) Carrell, C. J., Bush, L. A., Mathews, F. S., and Di Cera, E. (2006) High resolution crystal structures of free thrombin in the presence of K^+ reveal the basis of monovalent cation selectivity and an inactive slow form. *Biophys. Chem. 121*, 177−184.

(28) Pineda, A. O., Carrell, C. J., Bush, L. A., Prasad, S., Caccia, S., Chen, Z. W., Mathews, F. S., and Di Cera, E. (2004) Molecular dissection of Na^+ binding to thrombin. *J. Biol. Chem. 279*, 31842−31853.

(29) Bah, A., Garvey, L. C., Ge, J., and Di Cera, E. (2006) Rapid kinetics of Na^+ binding to thrombin. *J. Biol. Chem. 281*, 40049−40056.

(30) Vogt, A. D., Bah, A., and Di Cera, E. (2010) Evidence of the E*-E equilibrium from rapid kinetics of Na^+ binding to activated protein C and factor Xa. *J. Phys. Chem. B 114*, 16125−16130.

(31) Gianni, S., Ivarsson, Y., Bah, A., Bush-Pelc, L. A., and Di Cera, E. (2007) Mechanism of Na^+ binding to thrombin resolved by ultra-rapid kinetics. *Biophys. Chem. 131*, 111−114.

(32) Pozzi, N., Chen, R., Chen, Z., Bah, A., and Di Cera, E. (2011) Rigidification of the autolysis loop enhances Na^+ binding to thrombin. *Biophys. Chem. 159*, 6−13.
(33) Prasad, S., Wright, K. J., Roy, D. B., Bush, L. A., Cantwell, A. M., and Di Cera, E. (2003) Redesigning the monovalent cation specificity of an enzyme. *Proc. Natl. Acad. Sci. U.S.A. 100*, 13785−13790.
(34) Krem, M. M., Prasad, S., and Di Cera, E. (2002) Ser(214) is crucial for substrate binding to serine proteases. *J. Biol. Chem. 277*, 40260−40264.
(35) Galletto, R., Jezewska, M. J., and Bujalowski, W. (2005) Kinetics of allosteric conformational transition of a macromolecule prior to ligand binding: Analysis of stopped-flow kinetic experiments. *Cell Biochem. Biophys. 42*, 121−144.
(36) Halford, S. E. (1971) *Escherichia coli* alkaline phosphatase. An analysis of transient kinetics. *Biochem. J. 125*, 319−327.
(37) Fersht, A. R., and Requena, Y. (1971) Equilibrium and rate constants for the interconversion of two conformations of α-chymotrypsin. The existence of a catalytically inactive conformation at neutral pH. *J. Mol. Biol. 60*, 279−290.
(38) Papaconstantinou, M. E., Gandhi, P. S., Chen, Z., Bah, A., and Di Cera, E. (2008) Na^+ binding to meizothrombin desF1. *Cell. Mol. Life Sci. 65*, 3688−3697.
(39) Gombos, L., Kardos, J., Patthy, A., Medveczky, P., Szilagyi, L., Malnasi-Csizmadia, A., and Graf, L. (2008) Probing conformational plasticity of the activation domain of trypsin: The role of glycine hinges. *Biochemistry 47*, 1675−1684.
(40) James, L. C., and Tawfik, D. S. (2005) Structure and kinetics of a transient antibody binding intermediate reveal a kinetic discrimination mechanism in antigen recognition. *Proc. Natl. Acad. Sci. U.S.A. 102*, 12730−12735.
(41) Bae, S., Kim, D., Kim, K. K., Kim, Y. G., and Hohng, S. (2011) Intrinsic Z-DNA is stabilized by the conformational selection mechanism of Z-DNA-binding proteins. *J. Am. Chem. Soc. 133*, 668−671.
(42) Tang, C., Schwieters, C. D., and Clore, G. M. (2007) Open-to-closed transition in apo maltose-binding protein observed by paramagnetic NMR. *Nature 449*, 1078−1082.
(43) Rinnenthal, J., Buck, J., Ferner, J., Wacker, A., Furtig, B., and Schwalbe, H. (2011) Mapping the landscape of RNA dynamics with NMR spectroscopy. *Acc. Chem. Res. 44*, 1292−1301.
(44) van Holde, K. E. (2002) A hypothesis concerning diffusion-limited protein-ligand interactions. *Biophys. Chem. 101−102*, 249−254.